ELSEVIER

Journal of Nuclear Materials 283–287 (2000) 273–277

journal of nuclear materials

www.elsevier.nl/locate/jnucmat

Microstructures in Ti–Al intermetallic compounds irradiated at 673 K in HFIR

Y. Miwa [a,*], T. Sawai [a], K. Fukai [a], D.T. Hoelzer [b], A. Hishinuma [a]

[a] *Department of Materials Science and Engineering, Japan Atomic Energy Research Institute, Shirakata Shirane 2-4, Tokai-mura, Naka-gun, Ibaraki-ken 319-1195, Japan*

[b] *Metals and Ceramics Division, Oak Ridge National Laboratory, Oak Ridge, TN 37831-6376, USA*

Abstract

Four kinds of Ti–Al intermetallic compounds were made from powder metallurgical processing using mechanical alloying or plasma rotating electrode processing. One consisted of α_2-Ti_3Al single phase, and the others consisted of α_2-Ti_3Al and γ-TiAl duplex phases. These intermetallic compounds were irradiated at 673 K to the fluence of 5.16×10^{25} n/m^2 ($E>1$ MeV) in the high flux isotope reactor. After irradiation, transmission electron microscopy was carried out. Cavities were observed in both the α_2-Ti_3Al- and γ-TiAl-phases. The nucleation behavior of cavities in the α_2-Ti_3Al- and γ-TiAl-phases was influenced by chemical composition and fabrication processes.

1. Introduction

Ti–Al intermetallic compounds offer advantages of large strength-to-weight ratio and high strength and good oxidation resistance at elevated temperature. In the binary Ti–Al system, the α_2-Ti_3Al (α_2) and γ-TiAl (γ) are promising candidates for structural materials.

The contact dose rate of TiAl after 10-year-cooling [1] is about three times higher than that for recycling by remote handling, 25 mSv/h [2]. The contact dose rate of TiAl is about 10^4 to 10^6 times lower than those of F82H and 316SS [1], though that of V–4Cr–4Ti–0.1Si and SiC–SiC was about 1/3–1/20 of TiAl [1]. For application in future fusion nuclear systems, Ti–Al intermetallic compounds are one of the attractive materials due to lower contact dose rate.

Several papers have been published on the effects of electron irradiation [3,4], He^+ irradiation [4–7] and neutron irradiation [8,9] on Ti–Al intermetallic compounds. The ordered intermetallic compounds showed a superior resistance to void swelling under electron irradiation at 473–873 K [3,4], and good resistance to embrittlement after neutron irradiation at 873 K to 1×10^{24} n/m^2 ($E>1$ MeV) [8]. On the other hand, Song et al. [7] reported γ-TiAl showed a poor resistance of He bubble nucleation after He^+ irradiation to 2.9 dpa at room temperature. Kohyama et al. [9] reported TiAl consisting of both equiaxed γ-grains and α_2/γ lamellar grains showed a significant ductility loss with neutron irradiation to 8.5 dpa at 376–873 K. In this paper, we report the effect of neutron irradiation on microstructural changes in equiaxed α_2- and γ-grains focused on the cavity formation behavior.

2. Experimental procedure

The materials used in this study consisted of four kinds of Ti–Al intermetallic compounds, and were produced by powder metallurgical processing. The nominal chemical compositions and notations are listed in Table 1. The chemical composition for K1, K2 and K3 was calculated using the chemical composition of Al and Ti powders. The chemical composition of K4 was analyzed from the mother cast alloy. The average diameter of Ti and Al powders used for K1, K2 and K3 was about 30 μm. These powders were mixed to obtain the nominal

* Corresponding author. Tel.: +81-29 282 6082; fax: +81-29 282 6122.

E-mail address: miway@popsvr.tokai.jaeri.go.jp (Y. Miwa).

0022-3115/00/$ - see front matter
PII: S0022-3115(00)00357-3

Table 1
Nominal chemical compositions (at.%)

	Ti	Al	O	N	H
K1	65.78	31.49	1.49	0.17	1.08
K2	52.53	45.90	1.26	0.12	0.19
K3	49.30	48.11	2.31	0.19	0.09
K4	52.41	46.87	0.63	0.06	0.03

chemical compositions (Table 1), and then were mechanically alloyed in an Ar gas atmosphere for 720 ks using a stainless steel ball mill. The mechanically alloyed powders were isostatically hot pressed in vacuum under 176.8 MPa at 1373 K for 10.8 ks, and then annealed in vacuum at 1473 K for 36 ks. The powder used for K4 was prepared from cast mother alloys by the plasma rotating electrode process (PREP), and had an average particle diameter of about 250 μm. A cylindrically compressed powder was made by hot isostatic pressing under 176.8 MPa at 1323 K for 10.8 ks. This was followed by isothermal hot forging up to a reduction of 78% in height with a strain rate of 3.8×10^{-4} s^{-1} at 1223 K in vacuum.

TEM disks, 3 mm in diameter and 0.25 mm in thickness, were prepared by wire cutting. These TEM disks were irradiated at about 673 K in the high flux isotope reactor (HFIR) at the Oak Ridge National Laboratory. The resulting thermal and fast neutron fluences, taking into account the specimen position in the reactor were 1.83×10^{26} n/m^2 ($E<0.5$ eV) and 5.16×10^{25} n/m^2 ($E>1$ MeV), respectively, [10]. Displacement per atom (dpa) values for $Ti_{0.5}Al_{0.5}$ and $Ti_{0.75}Al_{0.25}$ were estimated by the NRT model using displacement energy of 27 eV for Al and 40 eV for Ti [11] and by a table of displacement damage-energy cross-section calculated by the SPECTER code [11]. The displacement damages for $Ti_{0.5}Al_{0.5}$ and $Ti_{0.75}Al_{0.25}$ were 11 and 9.8 dpa, respectively. The He production in Al was 6.42 appm [10]. The He production in Ti calculated using the Japanese evaluated nuclear data library, JENDEL-3.2 [12], was about 3.7 appm. The calculated He concentrations in $Ti_{0.5}Al_{0.5}$ and $Ti_{0.75}Al_{0.25}$ were 5 and 4.4 appm, respectively. After irradiation, transmission electron microscopy was carried out using a JEM 2000-FX microscope. The unirradiated specimens were also studied using a Phillips CM12 microscope equipped with an energy dispersive X-ray (EDX) analyzing system, VP9900.

3. Results

3.1. Unirradiated Ti–Al intermetallic compounds

Microstructures of the unirradiated Ti–Al intermetallic compounds are shown in Fig. 1. No lamellar structure was observed in all compounds. K1 consisted of a duplex structure of relatively larger matrix and smaller island grains, as seen in Fig. 1(a). The islands existed in matrix grains and along grain boundaries. In the islands, the concentration of Ti was higher than that in the matrix, and a higher number density of planar defects was observed. Both matrix and island grains were identified as the α_2-phase. K3 was designed to be a single γ-phase, but consisted of three phases of Al_2O_3, α_2 and γ. The γ-phase grains were larger than the α_2-phase grains (Fig. 1(b)). K2 and K4 consisted of two phases of relatively smaller α_2-phase and larger γ-phase grains (Figs. 1(c) and (d)). Twin boundaries were observed in the γ-phases in K1, K2 and K3. Dislocation lines and twin boundaries were observed in the γ-phases in K4. Pores were observed in grains and especially on grain boundaries of K1, K2 and K3, but not in K4. The average diameter and number density of pores among K1, K2 and K3 were about the same, and were 9.4–14.4 nm and $6–9\times10^{19}$ m^{-3}, respectively. Impurities such as Fe, Cr and Ni were detected in some of the α_2- and γ-grains of K2 and K3, and Ar was detected in the pores of K1 and K3. The details of microstructures in unirradiated specimens were presented elsewhere [13].

3.2. Irradiated Ti–Al intermetallic compounds

Figs. 2(a) and (b) show cavities observed in both the matrix and island grains of the irradiated K1, respectively. The faceted cavities were observed in both the matrix and island grains after irradiation. In the matrix, the cavities formed preferentially around pores within the range of about 75 nm from the surface of the pores. Some small cavities also formed far from pores. The distribution of cavities in the matrix was not uniform. In the island grains where a high density of planar defects was observed before irradiation, the cavities were smaller than in the matrix. The number density of cavities in the islands was much higher than that in the matrix. In the island, the cavities seemed to be arranged in rows, and few cavities were on the planar defects. On the grain boundaries between the matrix and island grains or between matrix grains, few cavities were observed. The size of cavities in both matrix and island grains was smaller than that of pores. The average diameter and number density of cavities in the matrix and

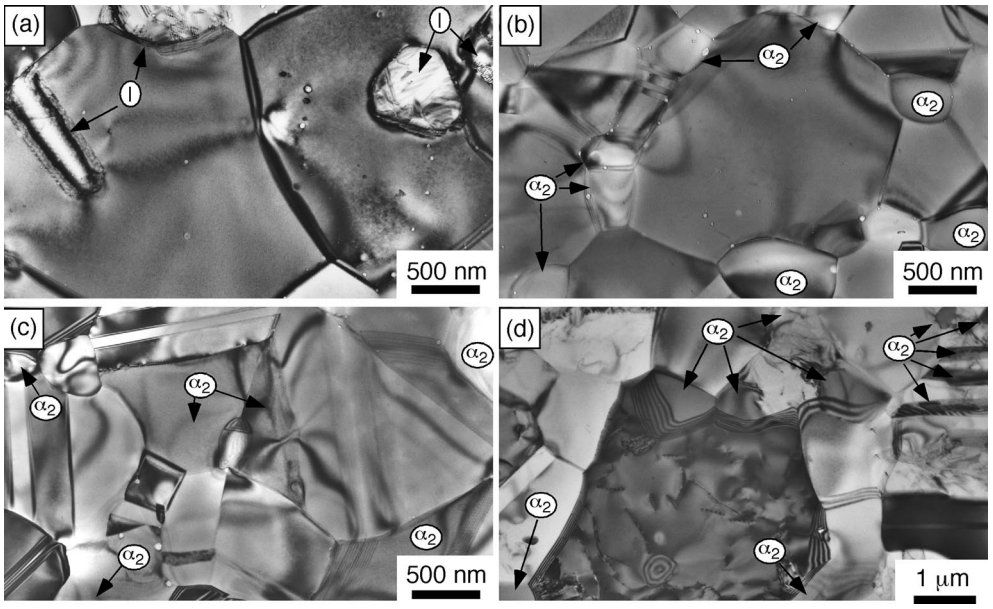

Fig. 1. Microstructures in unirradiated: (a) K1 (α_2-Ti_3Al); (b) K3 (α_2-Ti_3Al + γ-TiAl + Al_2O_3); (c) K2 (α_2-Ti_3Al + γ-TiAl); (d) K4 (α_2-Ti_3Al + γ-TiAl). In K1, islands were indicated by 'I', other grains were matrix. In K2, K3 and K4, α_2-Ti_3Al were indicated by 'α_2', and other grains were γ-TiAl.

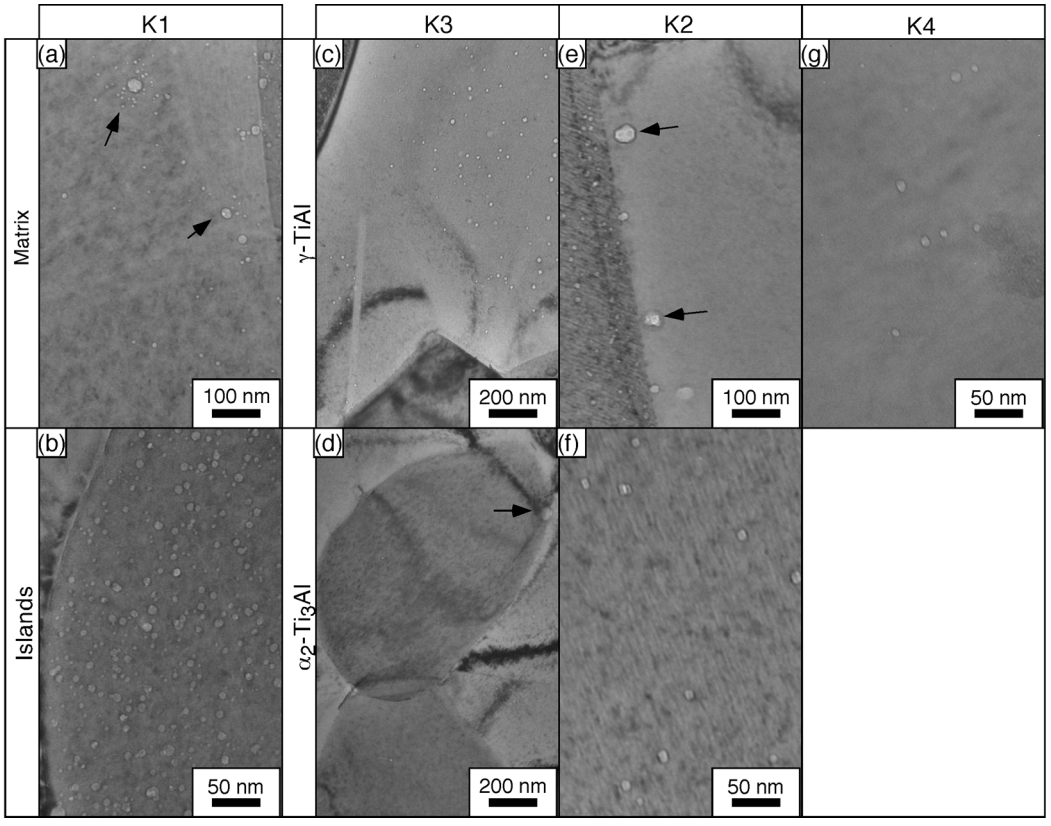

Fig. 2. Cavities in irradiated K1, K2, K3 and K4. Pores existed prior to irradiation are indicated by arrows. Microstructure in α_2 of K4 is not available.

island grains were 5.6 nm and 4×10^{20} m^{-3}, and 3.4 nm and 2×10^{22} m^{-3}, respectively. Swelling of matrix and island grains was 0.007% and 0.002%, respectively. Swelling of K1 was 0.007%.

In irradiated K3, small cavities were observed only in the γ-phase. Fig. 2(c) shows that the faceted cavities formed uniformly in γ-grains. There were cavity-free zones around γ–γ and γ–α_2 grain boundaries, and the width of the cavity-free zones was ~100 nm. However, only one γ–γ grain boundary where many cavities formed was observed. No cavities were observed around pores in γ-phase grains, which was different from the cavity nucleation behavior in the α_2-phase of K1. In the α_2-phase grains of K3, no cavities were observed, though many cavities occurred in α_2-phase grains of K1. The average diameter and number density of cavities in γ-phase were 9.4 nm and 2×10^{21} m^{-3}, respectively. Swelling of γ-phase was 0.03%. Swelling of K3 was 0.02%.

Figs. 2(e) and (f) show the cavities observed in both the γ- and α_2-phases in irradiated K2, respectively. Small cavities appeared in some γ-grains, but not in all the γ-phase grains. There were no cavities around pores in the γ-phase grains, which was similar to K3. There were no cavities on γ–γ grain boundaries, but there were some cavities on twin boundaries in the γ-phase grains. On the other hand, a higher density of small faceted cavities formed in α_2-phase grains (Fig. 2(f)). The cavities appeared around pores in the range of about 75 nm from the surface of the pores, which was similar to the cavity nucleation behavior observed in K1. The cavities also formed on α_2–γ grain boundaries (Fig. 2(e)). The average diameter and number density of cavities in α_2- and γ-phases were 5.7 nm and 1×10^{21} m^{-3}, and 17.5 nm and 4×10^{19} m^{-3}, respectively. Swelling of α_2- and γ-phases was 0.006% and 0.2%, respectively. Swelling of K2 was 0.2%.

In irradiated K4, only two γ-phase grains were studied because of its poor specimen condition by electropolishing. In these γ-phase grains, small cavities were observed after irradiation, as seen in Fig. 2(g). These faceted cavities formed along the dislocation lines which existed before irradiation. There were some cavities on twin boundaries in the γ-phase grain, but no cavities on grain boundaries. The diametrical size distribution of cavities in the γ-grains showed a bi-modal distribution [13]. The critical diameter of smaller cavities was 4 nm. The average diameter and number density of cavities in γ-phase were 5.6 nm and 8×10^{20} m^{-3}, respectively. Swelling of γ-phase was 0.006%.

In K1, K2 and K3, loop-shaped and dot-like clusters, about 10 nm in diameter, were observed in both the α_2- and γ-phases. In K4, stacking fault dislocation loops, about 50 nm in diameter, were observed along dislocation lines, twin boundaries and grain boundaries. Details were reported elsewhere [13].

4. Discussion

In the present work, faceted cavities were observed in the α_2- and γ-phases after neutron irradiation up to 11 dpa at 673 K. In K4, a bi-modal size distribution was observed for the cavities [13]. The larger faceted cavities in this bi-modal distribution are likely to be voids. Nakata et al. [4,5] observed similar large faceted cavities in α_2- and γ-phases damaged by He^+ irradiated up to 20 dpa at 773 K. Hishinuma et al. [3] and Nakata et al. [4], however, reported no void nucleation in either the α_2- or the γ-phase after 1 MeV electron irradiation up to ~30 dpa at 473–873 K. It is believed that void nucleation in Ti–Al ordered intermetallic compounds occurred under the cascade damage condition and/or gaseous element generation. It was expected that under neutron irradiation condition, the Ti–Al ordered intermetallic compounds also experienced void swelling.

In the α_2-phase of K1, K2 and K3, cavities formed in K1 (both the matrix and islands) and K2, but not in K3. In K1 and K2, the cavities formed preferentially around pores. The cavities were also observed far from pores. These pores existed prior to irradiation, and contained Ar gas. The range where cavities existed from the surface of pores was about 75 nm. It is suggested that Ar is recoiled from the pore by elastic collision with neutrons. The maximum recoil energy of Ar with 1 MeV neutron by elastic scattering was about 96 keV. The range of these energetic Ar ions in α_2-phase was calculated using TRIM 85, and was about 73 nm. This calculated range corresponded well to the measured range of cavities from the pore surface. Therefore the cavities around pores might be Ar gas bubble, or Ar gas might assist in the nucleation of cavities. In K3, however, cavities were not observed in either the α_2-grains or around pores in α_2-grains, even though the Ar gas was also detected in pores of K3. This means that the presence of Ar and other gases might be the key factor for the formation of cavities in the α_2-phase. In addition to Ar gas, He was generated from nuclear reactions of Al and Ti. The calculated He concentration in Ti_3Al was about 4.4 appm. Although He was produced in K3, cavities were not observed in its α_2-grains. Therefore the presence of He could not explain the difference in the cavity nucleation behavior. The reason that cavities were not observed in α_2-grains of K3 is not clear, but the alumina particles observed only in K3 may suggest an important role of solute oxygen. Although the nominal concentration of oxygen in K3 is almost twice as much as that of K1 or K2, almost all the oxygen in K3 is associated with these alumina particles, the volume fraction of which is about 3%. The concentration of solute oxygen seems to have an influence on swelling of α_2-phase in K1 (matrix), K2 and K3. Other impurities such as Fe, Cr and Ni were detected only in K2 but not in K1 and K3, which did not correspond to the nucleation behavior of cavities among them.

In the γ-phase, the cavities were observed in every specimen. However, there were differences in the nucleation behavior of cavities among K2, K3 and K4. In K2, the number density of cavities was much lower than in K3 and K4. In K3, the number density of cavities was the largest, and cavities formed uniformly in γ-grains. In K4, cavities were observed along dislocation lines that existed prior to irradiation. The size distribution of cavities in K3 and K4 looked like a bi-modal distribution [13]. In all the γ-grains investigated, there were no cavities near pores. Therefore the Ar gas in pores can be considered less effective in forming cavities in the γ-phase than in the α_2-phase. The calculated concentration of He in TiAl was about 5 appm. This amount is similar among K2, K3 and K4, which could not explain the difference of cavity nucleation behavior in γ-phase. Although the content of oxygen was highest in K3, almost all the oxygen was tied up with alumina, as discussed above. Oxygen also seemed to have an influence on swelling in γ-phase. However, the tendency for oxygen to affect the cavity nucleation in γ-phase seemed to be opposite to that in α_2-phase. Similar effects of gas atoms on cavity nucleation behavior in He^+ irradiation experiment were observed in [4,5]. In the range where almost all He^+ passed through and the He concentration was very low, the number density of cavities in γ-phase was larger than that in α_2-phase [5]. In the calculated projected range of He^+, where the He concentration was high, the number density of cavities in α_2-phase was larger than that in γ-phase [4]. It is speculated that the effect of gas atoms on the cavity nucleation behavior might be different between γ- and α_2-phases. Other impurities such as Fe, Cr and Ni were detected in K2 and K3 but not in K4. This did not correspond to the cavity nucleation behavior among them.

In He^+ implanted experiments [4,5], many cavities occurred on the γ–γ boundaries or γ–α_2 boundaries in K4. However, there were no cavities on grain boundaries after neutron irradiation. It is expected that irradiation conditions have a strong influence on the cavity nucleation site in Ti–Al intermetallic compounds.

5. Summary

Mechanically, alloyed or plasma rotating electrode processed Ti–Al alloys containing α_2-Ti_3Al- and γ-TiAl-phases were irradiated at 673 K to a fluence level of 5.16×10^{25} n/m^2 ($E > 1$ MeV). After irradiation, transmission electron microscopy was carried out.

Cavities were observed in the α_2-Ti_3Al- and γ-TiAl-phases. In the α_2-Ti_3Al-phase, cavities were observed around pores that existed prior to irradiation and contained Ar gas. But in the γ-TiAl-phases, no cavities were observed around the pores. The number density of cavities in α_2-Ti_3Al or γ-TiAl was different among specimens that had different chemical compositions and fabrication processes.

Acknowledgements

The authors are grateful to Mrs L.T. Gibson and A.T. Fisher for experimental support. This research was supported in part by an appointment (DTH) to the Oak Ridge National Laboratory Postdoctoral Research Associates Program administered jointly by the Oak Ridge National Laboratory and the Oak Ridge Institute for Science and Education. The research is sponsored by the Office of Fusion Energy Sciences, US Department of Energy, under contract DE-AC05-96OR22464 with Lockheed Martin Energy Research Corporation.

References

[1] Y. Seki, T. Tabata, I. Aoki, S. Ueda, S. Nishio, R. Kurihara, J. Nucl. Mater. 258–263 (1998) 1791.
[2] P. Rocco, M. Zucchetti, J. Nucl. Mater. 212–215 (1994) 649.
[3] A. Hishinuma, K. Nakata, K. Fukai, K. Ameyama, M. Tokizane, J. Nucl. Mater. 199 (1993) 167.
[4] K. Nakata, K. Fukai, A. Hishinuma, K. Ameyama, J. Nucl. Mater. 240 (1997) 221.
[5] K. Nakata, K. Fukai, A. Hishinuma, K. Ameyama, M. Tokizane, J. Nucl. Mater. 202 (1993) 39.
[6] O. Okada, K. Nakata, K. Fukai, A. Hishinuma, K. Ameyama, J. Nucl. Mater. 258–263 (1998) 1750.
[7] M. Song, K. Furuya, T. Tanabe, T. Noda, J. Nucl. Mater. 271&272 (1999) 200.
[8] A. Hishinuma, K. Fukai, T. Sawai, K. Nakata, Intermetall. 4 (1996) 179.
[9] A. Kohyama et al., in: Proceedings of the Second Japan/China Symposium on Materials for Advanced Energy Systems and Fission and Fusion Engineering, The University of Tokyo, Japan, 1994, p. 472.
[10] L.R. Greenwood, C.A. Baldwin, Fusion Reactor Materials Semiannual Progress Report, DOE/ER-313/23, 1997, p. 305.
[11] L.R. Greenwood, R.K. Smither, SPECTER: Neutron damage calculation for materials irradiations, ANL/FPP/TM-197, 1985.
[12] T. Nakagawa et al., J. Nucl. Sci. Technol. 32 (1995) 1259.
[13] Y. Miwa et al., Fusion Materials Semiannual Report, DOE/ER-313/26, 1999.